Eur. Phys. J. Plus (2024) 139:827
https://doi.org/10.1140/epjp/s13360-024-05570-9

THE EUROPEAN PHYSICAL JOURNAL PLUS

Technical Report

A detrended fluctuation analysis to examine the pollutant pattern over Gangetic West Bengal of India

Bidisha Halder[1], **Surajit Chattopadhyay**[2,a], **Goutami Chattopadhyay**[1]

[1] Department of Atmospheric Science, University of Calcutta, 51/2 Hazra Road, Kolkata 700019, India
[2] Department of Mathematics, Amity University, Kolkata, Major Arterial Road, Action Area II, Newtown, Kolkata 700135, India

Received: 31 January 2024 / Accepted: 20 August 2024

Abstract In this paper, we present the results of a careful investigation into the correlational pattern of various pollutants over Kolkata during the months before to the monsoon, which correspond to the pre-lockdown (2019) and lockdown (2020) periods. When Ozone, NO_x, SO_2, and surface temperature were subjected to detrended fluctuation analysis, we found that the SO_2 exhibits long-term positive autocorrelation in the 2019 pre-monsoon. However, during the lockdown, the Hurst exponent (H) dropped below 0.5, which led to the interpretation that the lockdown caused neighbouring pairs to transition between long-term high and low autocorrelation coefficients. Additionally, although the autocorrelation function for NO_x resembles a roughly sinusoidal pattern, lockdown has caused a change in H. Using H, fractal dimension and climate predictability, we have analysed the predictability behaviour of the pollutants and temperature under consideration.

1 Introduction

Air pollution poses a serious hazard to human life in India. According to Wikipedia (18 June 2021), it is thought to be the cause of the deaths of 2 million Indians per year. The main causes of the emissions of different air pollutants over the past two decades have been frequent industry, traffic expansion, urbanization, biomass burning, and population growth. Air pollution is a significant threat to human health in metropolitan areas and is getting worse [34, 72]. As a result of the significant amount of these contaminants that plants get, they are also significantly impacted by air pollution [33]. According to IQAir, a Swiss technology company, India, ranks 22nd out of the top 30 most polluted cities in the world as of March 17, 2021.

Different air contaminants are produced, transported, and diluted in large part due to meteorology [3]. The concentrations of air contaminants are significantly influenced by relative humidity (Kgabi et al., [35]). Aside from the current temperature, wind direction, wind speed, and precipitation can all have an impact on pollutants [4, 76]. According to Zhang et al. [76], temperature is positively connected with ozone while wind speed has a reverse correlation with contaminants. According to Banerjee et al. [4], the primary pollutant causing the decline in air quality was total suspended particle matter. In comparison with other pollutants, the concentration of NOx, CO, and SO_2 in the Gangetic region was high [37]. Different linear and nonlinear regressions were employed by Kayes et al. [34] in their study to examine the influence of climatic conditions on pollutants over Dhaka. They noticed a negative association between the amount of contaminants and both temperature and relative humidity. The complexity of Indian climate was discussed by Chattopadhyay et al. [12], and the neurocomputing approach was compared to statistical approaches.

Globally, the COVID-19 pandemic has had an impact. In December 2019, this first surfaced and then increased in some parts of the world [66]. Full or partial lockdowns have been decided in many nations [21]. Even if the epidemic has numerous detrimental effects on both human health and the environment, it also improves air quality [22]. Air quality is used to understand the current level of air pollution and how it affects the environment [48]. The impact of the shutdown on aerosol optical depth over India was investigated by Gautam [22]. On March 23, 2020, a curfew was imposed over Gangetic West Bengal and was later extended. According to satellite data and more than 10,000 air quality stations, the lockdown phase decreased global economic and transportation activity, which in turn decreased ground-level air pollution concentrations [74]. The air quality over Kolkata and Howrah was monitored by Sarkar et al. [62] both before and after the lockdown. They employed several statistical analyses, used co-relational matrices to understand the variance of the air contaminants, and used GIS-based methodologies for their study.

Atmospheric ozone is distributed in three layers of the atmosphere—troposphere, stratosphere and mesosphere. Due to human activity ozone concentration has been increasing in the lower atmosphere, i.e., troposphere but decreasing in the stratosphere (Checa et al., [15, 19]). Stratospheric ozone is known as 'Good Ozone' as it absorbs harmful ultraviolet radiation, whereas tropospheric ozone is known as 'Bad Ozone' as it plays the role of a pollutant. Tropospheric ozone, 10% of the total ozone, is a minor constituent but

[a] e-mails: surajitchatto@outlook.com; schattopadhyay1@kol.amity.edu (corresponding author)

plays a very important role in cycling minor species (Ghosh et al., [23]) emitted by different natural and anthropogenic processes[20]. The tropospheric ozone is a greenhouse gas which is produced by photochemical reaction [39, 58] and is unhealthy to plants and humans [29]. During photochemical processes, the NOx emissions lead to high ozone concentrations [20]. Kgabi et al. [35] in their study observed the concentration of tropospheric ozone and relate it with other meteorological conditions. To estimate the ozone concentration in an urban city Abdul Aziz et al. [1] used an artificial neural network model. In the megacities like Delhi Ozone and PM 2.5 are the two most important pollutants observed by Chen et al. [17]. They put down a quantitative analysis depicting the effects of mitigation strategies on both ozone and particulate matter. Jana et al.[28] reported that during pre-monsoon months tropospheric ozone attained maximum value and during monsoon it attained minimum over India except for Shimla and Srinagar. For such variations, they suggested chemical explanations. Reddy et al. [56] also reported the same in their study. They showed during pre-monsoon months the higher surface temperature leads to higher photochemical production and during monsoon, the higher relative humidity gives a negative correlation between temperature and ozone. Londhe et al. [43] examined the diurnal cycle of ozone which became maximized at noon and minimized at sunrise. During the lockdown period, Bera et al. [6] observed the UV index which is related to the tropospheric ozone over Kolkata, Delhi, Mumbai, and Chennai—four megacities of India.

Jana et al. [27] reported that the average temperature had an important influence on tropospheric ozone over Alipore, Kolkata. Gunther et al. [25] also studied the correlation between daily maximum ozone and temperature over Pune. Rathore et al. [59] used satellite and ground-based data to assess the seasonal and inter-annual variability, long-term trends, and radiative forcing of tropospheric column ozone (TPO) in India from 2005 to 2020. The investigation by Rathore et al. [59] reveals an extremely high yearly averaged TPO in the Indo-Gangetic Plain (IGP) and North West India, approximately 45–50 DU. Kothawale et al. [38] showed fluctuations in daily temperature in India in the pre-monsoon months and reported that it is the hottest season of the year and during this season the daily high temperature affects human comfort. Roberts [57] in his work studied the relationship between daily mean temperature and the air pollutants. Hu et al. [32] had shown that PM10 and ozone influence heat-related all-cause and non-accidental mortality, implying that policymakers should consider air pollutants when developing heat-health warning systems and also stated that future studies with similar designs and settings are required. Maithani et al. [45] studied the lockdown effect on surface temperature over Dehradun. Temperature, NOx, PM2.5—these parameters have a crucial role in the long-running process of transmission of COVID-19[41]. Shahzad et al. [64] observed the impact of atmospheric temperature on COVID in some cities of China. The result has shown a positive correlation between temperature and COVID in some cities of china while in some cities they got a negative correlation and others show mixed trends. These variations among different regions can be justified by the differences in the factors like number of COVID-19 cases, health infrastructure in that region, atmospheric temperature, etc. Ogaugwu et al. [51] studied the relation of COVID-19 with temperature and relative humidity. They found a weak correlation between temperature and COVID, but no significant relation was observed between humidity and COVID-19 transmission.

Chattopadhyay et al. [10] reported that tropospheric ozone depends on NOx, PM10, and SO_2 during the summer monsoon over Kolkata. Chakraborty et al. [9] in their work calculate the total emissions of different greenhouse gases like SO_2, NO, etc., from the thermal power plants over India. These SO_2 and NO_x can be transformed into sulphate and nitrate substances and then transported for several miles. Both NO_x and SO_2 are harmful to human beings. They are responsible for lung infections, irritation in the eyes, headaches, asthma, etc. Bhanarkar et al. [7] worked on the emission of NO_2 and SO_2 from various sources like domestic, industrial, and vehicular over Jamshedpur, India, and trying to know about the pollution loads on the environment. Their analysis showed that 77% of SO_2 and 68% of NO_2 that is more than 50% of these pollutants are directly emitted from industries only succeeded by vehicular and domestic sources over that region.

The brownish gas NOx is mainly produced by combustion of fossil fuels from vehicles and power plants (Kgabi et al., [35]). It is also produced naturally from lightning. In atmospheric chemistry, NO_x is a general term which primarily indicates the two pollutants—nitric oxide and nitrogen dioxide. Pudasainee et al. [55] showed an inverse relationship between NOx and ozone. During pre-lockdown periods an anti-correlation between NOx and ozone indicates higher Ozone production with decreasing NO_x [53]. Observing surface ozone and nitrogen oxides are important to understand the variation and impact of trace gases. In pre-monsoon period the NO_x concentration is increased due to the lightning activity than in the monsoon period which further affects the surface ozone [54]. Vadrevu et al. [71] in their work showed that NO_2 was reduced by about 13% during the lockdown period (25th March–3rd May 2020) than the phases (1st January–24th March 2020). They also reported that NO_2 was reduced by 19% during the 2020 lockdown than the same period in 2019. Tyagi et al. (March, [69]) have analysed the seasonal variation of NO_x and ozone over north-eastern India and they suggested that ozone contributes to transport pollutants. Ghude et al. [24] used the diurnal and seasonal variation of NO_2 to recognize the principal NOx sources over the Indian subcontinent.

SO_2 is a toxic colourless gas with a choking odour. Sulphur has both natural and anthropogenic sources. SO_2 is mainly emitted from the combustion of fossil fuel, and power plants and the natural source of SO_2 is volcanic activity which emits large amount of sulphur dust into the atmosphere. Over the northern part of India Mallik et al. [46] used the modern satellite observatory system to estimate the high concentration of SO_2 which is generally carried out from Africa. One of the largest emitters of SO_2 is India [47]. Hence, to know the level of air pollution in India and mitigate it we should focus on the emission of SO_2. Lu et al. [44] in their study showed that during 2005–2012 SO_2 emissions increased notably by 71% over the coal-fired power plants of India. Kharol et al. [36] in their recent work showed a large SO_2 hotspot in India is at Morbi, Gujarat. At present the SO_2 emitted from the ceramic industry Morbi is five times more than in 2005. Kayes et al. [34] in their study observed that SO_2 concentration is increasing in air over Dhaka. SO_2 concentration is high at the time of pre-monsoon months than monsoon and winter time over the region of central

Himalayas— studied by Naja et al. [50]. During the pre-monsoon months the higher concentration of SO_2 indicates that air masses are transported from the Indo-Gangetic Plain (IGP) region which is full of industries and power plants. In spite of taking various steps in order to reduce the SO_2 emissions, it is not completely under control. So Cofala et al. [18] tried to optimize and limit the SO_2 emission in a cost-effective way. This optimization procedure has potential to eradicate the threat of sulphur deposition without any harm to animals and vegetations in an inexpensive way.

Mirzaei et al. [49] studied the statistical analysis of the trend of variations of different air pollutants (SO_2, ozone, and NOx) over Iran. Liu et al. [42] showed the relationship between ozone and its sources by using coupling detrended fluctuation analysis (DFA). They reported a complex nonlinear feature was exhibited by ozone and its precursors in the atmosphere. Chelani [16] used DFA method to study the air pollutant concentration which exceeds the threshold value. Padma et al. [52] reported a comparative study of the behaviour of the tropospheric ozone concentration over Chennai and showed the Hurst exponent of surface ozone has anti-persistent behaviour. Kalamaros et al. [30] examined the temperature time series over Greece by using multifractal DFA and showed a multifractal behaviour of time series. Roy et al. [58] showed how ozone and its precursors are seasonally distributed at the boundary layer and for this, they used the chemical transport model over the Indian region for the first time. In recent work, Chattopadhyay et al. [11] reported a comparative study between different neuro-computing approaches for generating predictive models for ozone, NOx, SO_2 and PM10 over Gangetic West Bengal during pre-monsoon season.

The higher the level of air pollution, the greater the risk for human health. But the critical pandemic situation constrained regular activities and confined human beings in isolation, which reduced a great amount of pollution, and turned out to be a healing period for the environment [5]. [68] observed during the initial phase of the lockdown ozone was low but with the growth of lockdown phases, it gradually increased. They also noticed that during the lockdown the concentrations of particulate matters also reduced by about half compared to previous year and reported that in lockdown NO_2, CO, NO concentrations showed significant reduction. During the lockdown periods, numerous precipitation events over the Bay of Bengal due to depression showed a significant reduction in the primary pollutants over Bhubaneswar [53]. In the former way of research, it was a convention to study air pollution and monsoon separately, but according to modern observations, those two have an underlying connection and hence require to be studied accordingly [40]. Singh et al. [67] reported the non-uniform variation of air pollutants over Chennai during COVID-19 phases. Sathe et al. [63] showed a significant reduction of NO_2 by 46–61%. In another recent work, Karuppasamy et al. [31] studied the improvement of the quality of the air during the lockdown period of India. Shehzad et al. [65] and Allu et al. [2] also reported the same observation in their work. Not only in India, but also in Wuhan (China), Milan(Italy), and New York (USA) similar trend is observed in the reduction of air pollutant concentrations resulting from the global pandemic[8]. [5] examined the air quality over Kolkata during and before this pandemic and observed the variation of air pollutants like NO_2, ozone, SO_2, CO, $PM_{2.5}$ and PM_{10}. Allu et al. [2] in their recent work observed the same pattern of air quality over Hyderabad and they used the Pearson correlation coefficient to correlate the concentration of ozone with other pollutants. Rupakheti et al. [61] studied the concentration of different pollutants to know the amount of air pollution over Lumbini, a region along the Himalayan foothills.

In the view of the above literature survey, we have adopted a methodology to understand the variation of any possible intrinsic pattern of different pollutants (SO_2, ozone, and NOx) and the meteorological parameter temperature over Gangetic West Bengal during pre-lockdown and lockdown periods (i.e. 2019 and 2020). The detailed methodology will be discussed in the subsequent section.

2 Methodology

The methodology presented in this work consists of:

1. Autocorrelation function,
2. Detrended fluctuation analysis and
3. Computation of Hurst exponent.

The data for this methodology are taken from Central Pollution Control Board, India, and the website is: http://www.cpcbenvis.nic.in/.

2.1 Autocorrelation function

Many stochastic systems include both a random component and predictability between individual elements. The autocorrelation function in statistics, which measures the correlation between a data set and its shifted form, can occasionally be used to explain this. One way to gauge how well a previous value can forecast a future value is to look at its autocorrelation. First we have performed autocorrelation analysis on the concentration of different pollutants like ozone, NOx, SO_2 and the meteorological parameter temperature during the pre-monsoon months from May to mid-June in the year of 2019 and 2020, i.e., during the pre-lockdown and the lockdown periods. The autocorrelation coefficients can be determined by [75]:

$$r_k = \frac{\mathrm{Cov}(x \text{ first}(n-k), x \text{ last}(n-k))}{\sqrt{\mathrm{Var}(x \text{ first}(n-k))}\sqrt{\mathrm{Var}\ (x \text{ last}(n-k))}} \tag{1}$$

Here, r_k describes the autocorrelation of order k, x_{first} (n-k) and x_{last} (n-k) represents the first (n-k) and last (n-k) data values, respectively, and k ranges from k = 1…n. All the values of autocorrelation coefficients that can be determined from a time series are named autocorrelation function (ACF).

In this study, up to 20 lags we calculate the autocorrelation coefficients and the graphs corresponding to both years are given below.

2.2 Detrended Fluctuation Analysis (DFA)

The self-similarity of a random process implies the preservation of the law of distribution in varying time scales. A stochastic process is self-similar when it is described by the same finite-dimensional distribution satisfied by the original stochastic process. The method of detrended fluctuation analysis (DFA) implies a method to study the scaling behaviour of a time series. It was introduced by Peng et al. (1994). Subsequently, the method got significant popularity in the study of long-range correlations. In the present work, we consider time series about SO_2, NOx, ozone and temperature that are collected for the months from March to June for the years 2019 and 2020. We apply DFA to each of the time series for each year. Throughout the study we consider the time series data as x_k of length N. To implement DFA we start with the calculation of the mean of the entire time series data as follows:

$$\langle x \rangle = \frac{1}{N} \sum\nolimits_{k=1}^{N} x_k \tag{2}$$

The mean is then subtracted from the entries of the time series to eliminate the global trend of the data. This will create a different set of data points that will help us to construct a profile as a cumulative sum of the resultant data set obtained. Mathematically saying, the profile is:

$$\chi_i = \sum\nolimits_{k=1}^{N} x_k - \langle x \rangle \tag{3}$$

Further scaling analysis will be implemented on the profile χ_i and this will help us to remove any prior assumption of the stationary of the data. Thereafter, we partition the profile into $s_N. = \mathrm{Int}\left(\frac{N}{s}\right)$ non-overlapping segments of equal time scale S. If N is not divisible by S then there will be some left out data. To bring the left-out data into our computation we repeat the same procedure from the end. Therefore, we have two N_S segments for a given time series if the time scale does not divide the total length of the time series. However, if S divides then we need exactly N_S non-overlapping segments. A linear trend is fitted to each segment, and the local trend is then subtracted from each profile. In this way, the process of detrending is computed under the preview of DFA.

2.3 Hurst exponent (H)

Rescaled range analysis, first introduced by Hurst in 1951, has been widely utilized to analyse the persistence and long-term dependence of natural time series. Hurst et al. [26] employed rescaled range analysis to predict long-term storage for Egypt's Aswan dam reservoir. Rescaled range analysis and other sophisticated methods are commonly used to evaluate and analyse persistence and long-term memory in real-world data across several areas. A random process with some degree of autocorrelation is known as a long memory process. River flow shows this type of long-term reliance (Rehman and Siddiqi, [60]). Hurst, a hydrologist, studied reservoir modelling for the Nile River. The Hurst exponent, which can be computed using the wavelet method and has diverse uses, is named after him. Hurst exponent applications have gained popularity among researchers in various domains, including stock trends, oil well logs, computer network traffic, geophysical investigations, hydrological difficulties, and meteorological time series analysis (e.g. Devi and Chattopadhyay, [13, 14]).

The Hurst exponent (H) is related to the autocorrelation of the time series and indicates the rate at which they decrease with the increasing lag. This is also referred to as the index of long-range dependence. If Hurst exponent (H) lies between 0.5 and 1, it is interpreted that the time series is characterized by long-term positive autocorrelation. This implies that a high value in the time series is most likely to be followed by another high value. If Hurst exponent (H) is below 0.5 we understand that the time series is characterized by long-term switching between high and low values in adjacent pairs. This implies that a high value will probably followed by a low value and this tendency will last a long time into the future. To calculate Hurst exponent (H) we have adopted detrended fluctuation analysis (DFA) method in this present work. When the Hurst exponent exceeds 0.5, the time series exhibits long-term memory and is likely to endure. This does not necessarily mean that the series is predictable. To ensure predictability, the Hurst exponent should be bigger than 1 for both the overall time series and its sublevels. Without this, the time series' fractal self-similarity properties will be less noticeable, resulting in uncertainty in prediction (Rehman and Siddiqi, [60]).

Table 1 Hurst exponent H from Fig. 1 corresponding to the pre-monsoon prior to lockdown

Variable	Hurst exponent	Remark	Fractal dimension D = 2 − H	Climate predictability index (PI) = 2 |D–1.5|
NOx	1.037	H is approximately 1. It indicates the predictability of the time series	0.963	1.074
SO_2	0.743	H is greater than 0.5, indicating that the time series has a long-term positive autocorrelation	1.257	0.486
Ozone	0.905	H is close to 1. It indicates the predictability of the time series	1.095	0.81
Temperature	0.484	H is less than 0.5, indicating that the time series is characterized by long-term switching between high and low values in nearby pairs	1.516	0.032

Table 2 Hurst exponent H from Fig. 2 corresponding to pre-monsoon within lockdown

Variable	Hurst exponent	Remark	Fractal dimension D = 2 − H	Climate predictability index (PI) = 2 |D–1.5|
SO_2	0.352	H is less than 0.5, indicating that the time series exhibits long-term flipping between high and low values in adjacent pairs	1.648	0.296
NOx	0.786	H is less but closer to 1 than SO2, indicating better predictability than SO2	1.214	0.572
Ozone	0.041	H is near to zero, indicating that the time series is exceedingly unpredictable	1.959	0.918
Temperature	0.151	H is significantly less than 0.5, indicating that the time series is exceedingly unpredictable	1.849	0.698

3 Results and discussion

From Table 1, it is clear that Hurst exponent (H) is greater than 1 for NOx and ozone. The values of Hurst exponent are 1.037 and 2.220, respectively, which indicate that during the pre-monsoon 2019 NOx and ozone have time series characterized by non-stationary. It is observed that α is greater than 0.5 for SO_2. Therefore, the generalized Hurst exponent is 0.743 and the time series is considered to be a fractional Gaussian noise. The Hurst exponent (H) value for temperature is $0.484 < 0.5$ which implies the time series is characterized by long-term switching between high and low values in adjacent pairs. Hence, we understand that the time series of SO_2 is having long-term positive correlation. This means that when there is no lockdown the high concentration of SO_2 is expected to be followed by high concentration of itself. Table 1 shows that NOx has a value of 1.037, indicating that H is close to one. It demonstrates the predictability of the time series. Furthermore, SO_2 displays a long-term positive autocorrelation ($H = 0.743 > 0.5$). However, the ozone H value is 0.905, which is near to 1. It demonstrates the predictability of the time series. Temperature's H is 0.484, which is less than 0.5, indicating long-term swinging between high and low values in close pairs. Table 2 shows that SO2 has a value of 0.352 when H is less than 0.5, showing long-term flipping between high and low values in nearby pairings. Additionally, NOx has a value of 0.786, bringing H closer to one and indicating improved predictability. Ozone has a value of 0.041 and H is close to zero, indicating high variability in the time series. Temperature has a Hurst exponent of 0.151, which is less than 0.5, indicating a very unstable time series. Comparing the results in Tables 1 and 2, we observe that NOx is non-stationary when there is no lockdown. However, during lockdown, it is represented by time series with long-term positive correlation.

Fig. 1 Scatter diagram of H **a** for NOx, **b** SO_2, **c** Ozone and **d** Temperature in the year of 2019

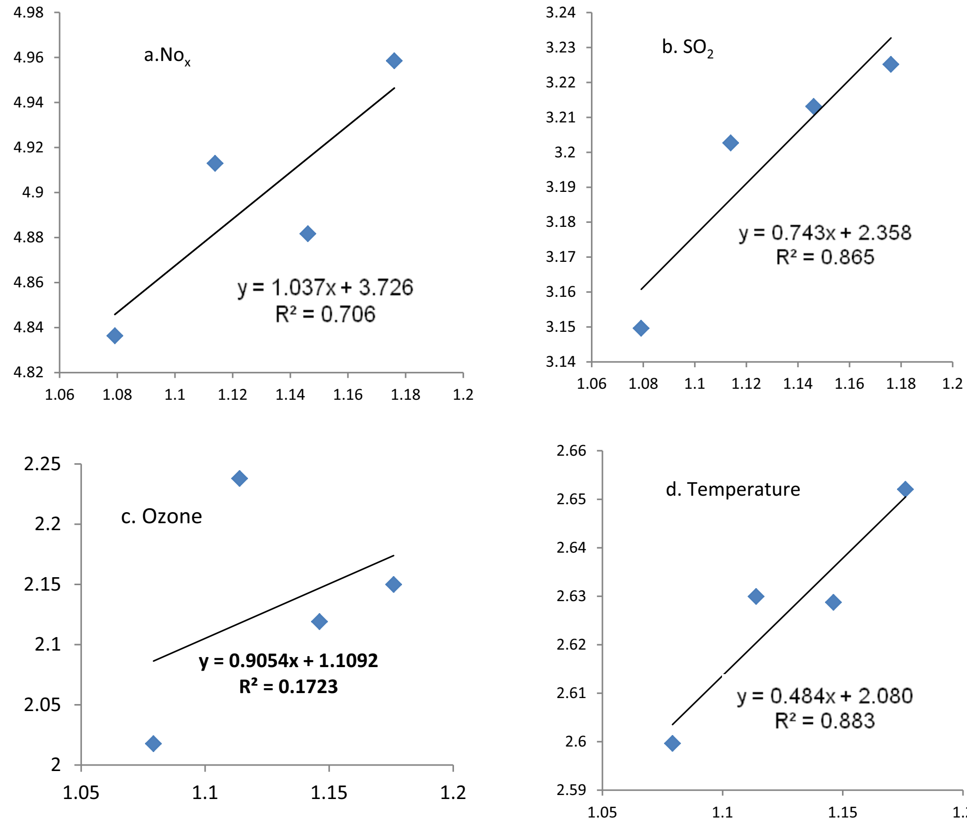

In both the tables, we have also displayed fractal dimension. The fractal dimension is a numerical measure of an object's roughness. Consider a fractional dimension between one and two dimensions of a straight line or plane. [70] and Viscek [73] provide thorough discussions on fractal dimensions. A relationship between Hurst exponent (H) and fractal dimension (D) is given by D = 2-H. If the fractal dimension D of the time series is 1.5, we get the standard Brownian motion. There is no association found between amplitude changes over two time intervals. The time series shows no discernible pattern in amplitude, making the process unpredictable. The process becomes predictable and persistent as the fractal dimension reduces to 1.0. Table 1 shows that during the pre-monsoon period before shutdown, the temperature has a D value of roughly 1.5. Because the time series' fractal dimension D is 1.5, we obtain the typical Brownian motion, suggesting that no relationship exists between amplitude changes over two time periods. The temperature time series exhibits no clear pattern in amplitude, rendering the procedure unpredictable. Ozone and NOx, on the other hand, have a fractal dimension of around one. Thus, ozone and NOx levels can be considered as persistent and predictable over the pre-monsoon period before lockdown. As the fractal dimension goes from 1.5 to 2.0, the process demonstrates anti-persistence. This means that a decrease in amplitude leads to an increase in the future or past. As a result, predictability increases once again. The scale-independent unit ensures predictability in the action process.

4 Concluding remarks

In the sections presented before, we have reported a rigorous study of the correlational pattern of some pollutants over Kolkata in the pre-monsoon months corresponding to the pre-lockdown and lockdown periods. Pre-monsoon months over Gangetic West Bengal are characterized by severe thunderstorms that have made the pre-monsoon periods very crucial for meteorological studies. The COVID-19 outbreak has had a significant impact on the life and economy of Kolkata which is our study zone. The role of pollutants in the genesis of atmospheric processes is well documented in the literature. Given that we have reported a thorough analysis of some significant pollutants and surface temperature in the pre-monsoon season corresponding to 2019 and 2020. To fight the pandemic lockdown was announced in the middle of March 2020 over Kolkata and this lockdown was continued till post-monsoon. As a consequence, almost the entire pre-monsoon of 2020 falls within the lockdown period. During this period, number of vehicles over the roads of Kolkata was reduced to its minimum and many factories in the surrounding region stopped

Fig. 2 Scatter diagram of H **a** for SO_2, **b** NOx, **c** Ozone and **d** Temperature in the year of 2020

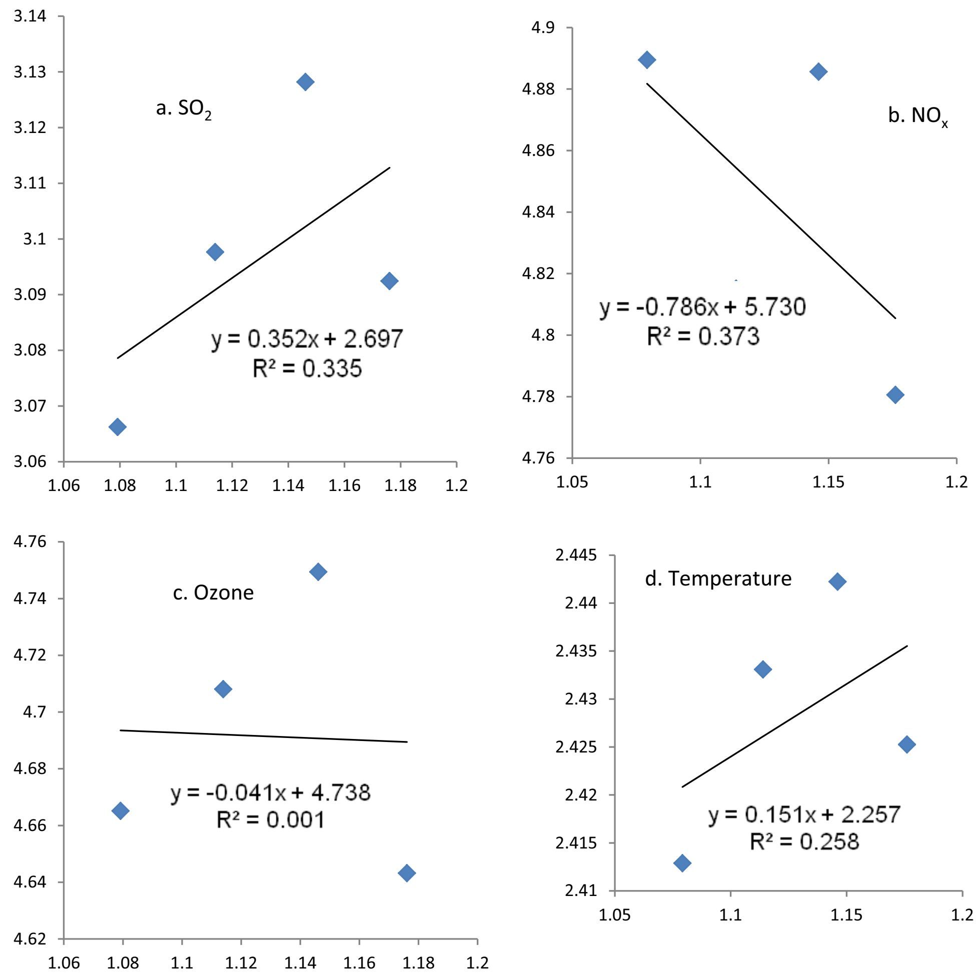

their regular functioning. Consequently, emissions of different pollutants experienced a significant reduction. In view of this, we have tried to understand the autocorrelational pattern of some important pollutants pertaining to 2019 and 2020.

Initially, we have exhibited the autocorrelation. For ozone, we have observed that during lockdown there is a very slow change in the autocorrelational pattern (please see Fig. 3 and Table 3) contrary to what happened in 2019 when there was no lockdown. Furthermore, in Fig. 3b, we have observed that ozone is highly persistent with a very high lag 1 autocorrelation coefficient. Figure 3b further shows that even in lag 15 the autocorrelation is close to 0.5. From this, we can interpret that the ozone concentration has a significant reduction in randomness due to lockdown. If we look at Table 2, we observe that Hurst exponent (H) is close to zero and hence the time series comes out to be stationary with long-term switching between high and low values; on the contrary, before lockdown it is showing random changes leading to the non-stationary time series. It may be interpreted that the lack of pollution due to the lockdown has a significant impact on ozone concentration. If we look at NOx, we observe that before and during lockdown

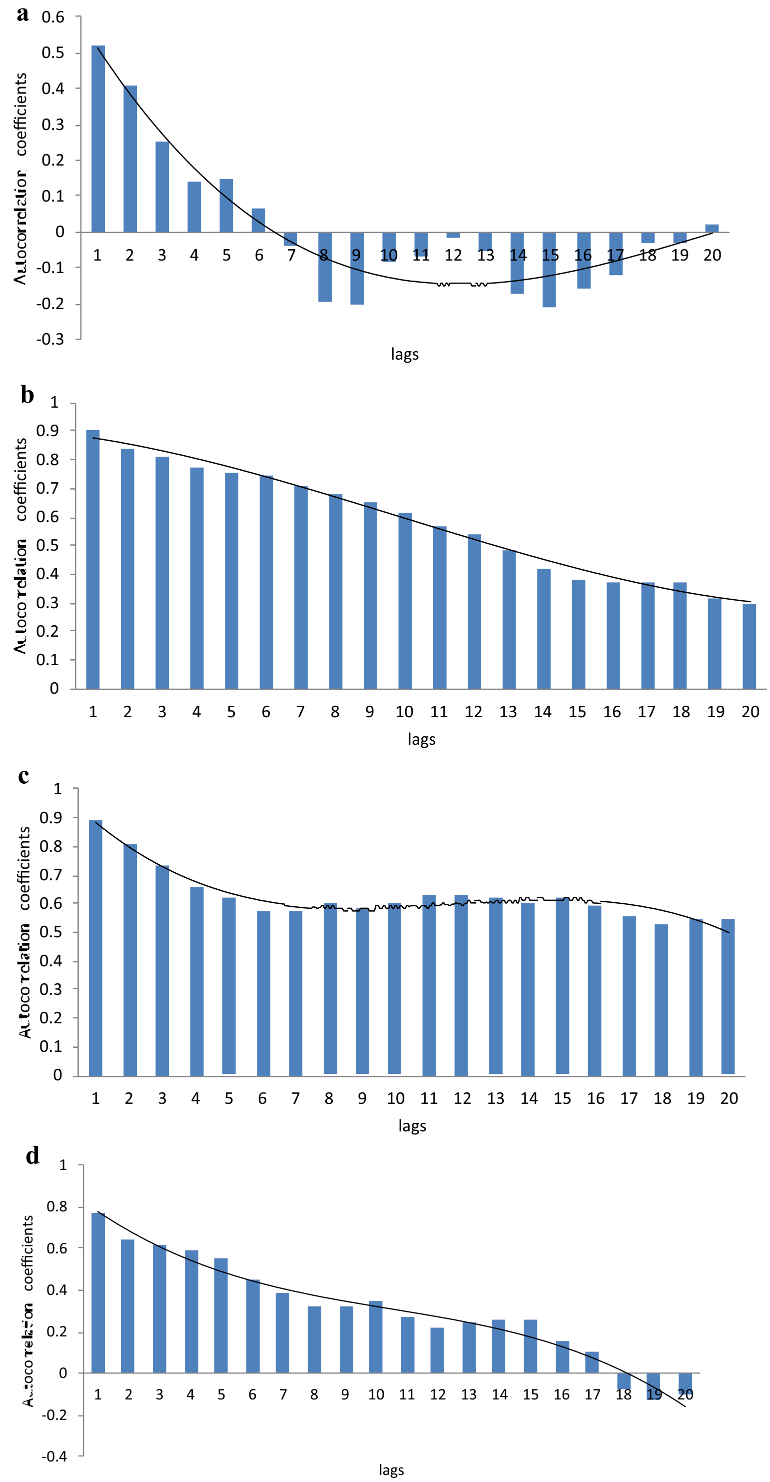

Fig. 3 **a** Autocorrelation function of ozone during pre-monsoon in 2019. **b** Autocorrelation function of ozone during pre-monsoon in 2020. **c** Autocorrelation function of temperature during pre-monsoon in 2019. **d** Autocorrelation function of temperature during pre-monsoon in 2020. **e** Autocorrelation function of NOx during pre-monsoon in 2019. **f** Autocorrelation function of NOx during pre-monsoon in 2020. **g** Autocorrelation function of SO_2 during pre-monsoon in 2019. **h** Autocorrelation function of SO_2 during pre-monsoon in 2020

the autocorrelation function has an approximate sinusoidal pattern (Fig. 3e and f). However, for NOx, there is a change in Hurst exponent (H). It is due to the lockdown. The non-stationary NOx time series has become a time series characterized by long-term positive autocorrelation.

However, for SO_2, we find a different kind of change. Prior to lockdown, the SO_2 was characterized by long-term positive autocorrelation. However, during lockdown, we get Hurst exponent (H) below 0.5 and hence we can interpret the lockdown has resulted in long-term switching high and low autocorrelation coefficient in adjacent pairs. However, for temperature, we do not find a very significant change in the long-term autocorrelation structure due to the call of lockdown. In Table 1, we observe that for the

Fig. 3 continued

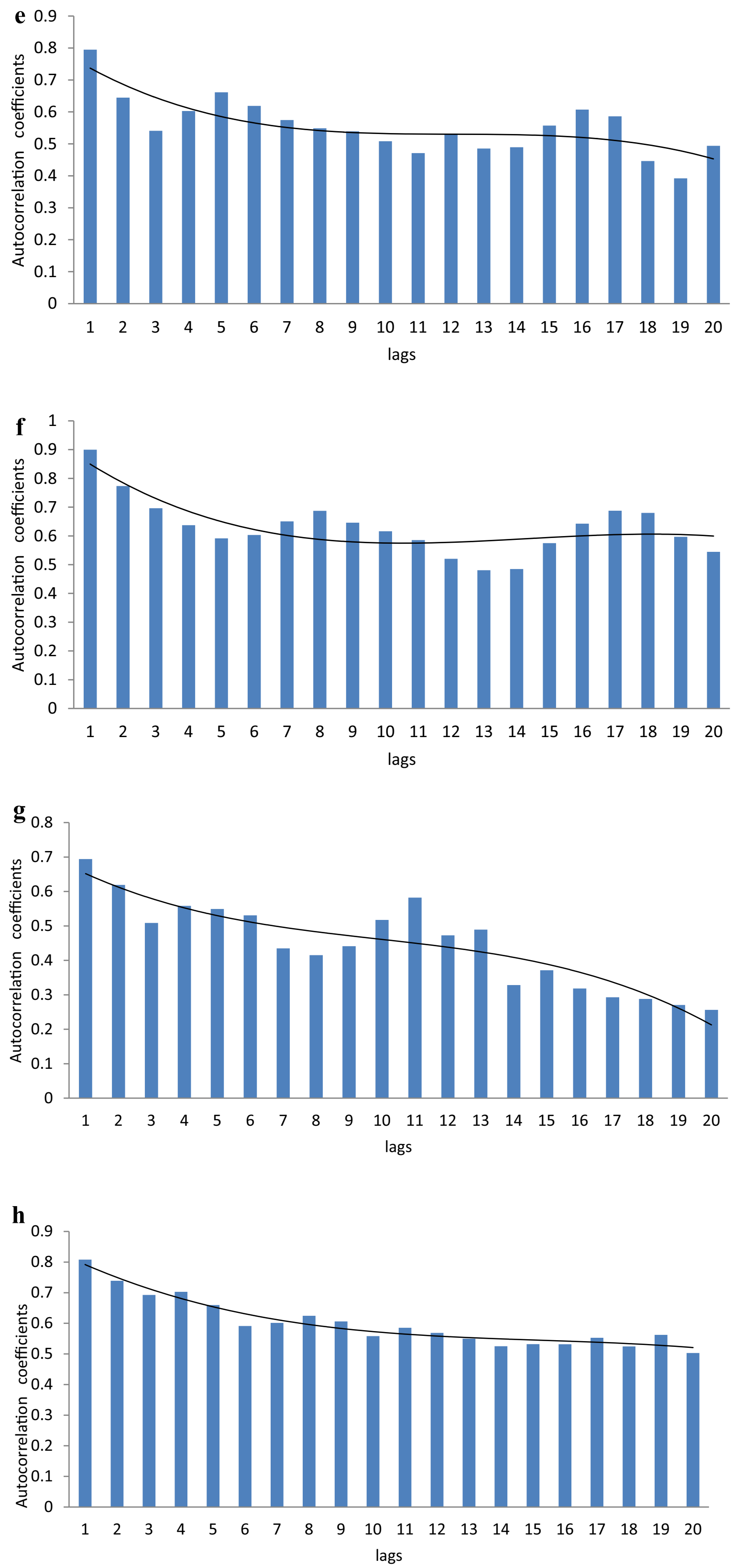

temperature time series, the fractal dimension is approximately 1.5. Hence, we can say that prior to lockdown, the temperature time series gets Brownian motion. In this case, there is no correlation between amplitude changes corresponding two successive time

Table 3 Tabular presentation of a comparative study of autocorrelation structure for NOx, SO_2, Ozone and Temperature before and during lockdown

Pollutants	Before lockdown (2019)	During lockdown (2020)
Ozone	Fractal dimension lies between 1 and 1.5	Fractal dimension is close to 1
NOx	Fractal dimension is close to 1. The process is predictable and exhibits persistence	Fractal dimension lies between 1 and 1.5. The process is anti-persistent
SO_2	Fractal dimension is less than 1.5	Fractal dimension lies between 1 and 1.5. The process is anti-persistent
Temperature	Fractal dimension is greater than 1.5. It is anti-persistent and a decrease in amplitude of the process is more likely to lead an increase in the future or past	Fractal dimension is greater than 1.5. It is anti-persistent and a decrease in amplitude of the process is more likely to lead an increase in the future or past

intervals. Therefore, no trend in amplitude can be discerned from the time series and hence the process is unpredictable [60]. In Table 1, we also find that, for NOx, the fractal dimension is close to 1 and hence the time series is interpreted to be persistent and hence predictable prior to the lockdown. Observing Tables 1 and 2, we observe that the fractal dimension is greater than 1.5. It is anti-persistent and a decrease in the amplitude of the process is more likely to lead an increase in the future or past. From both the tables, the climate predictability indices of ozone are found to be close to 1. However, with a closer look at H, we have observed that before lockdown, H is close to 1, which indicates the predictability of the time series. On the contrary, during lockdown, H is near to zero, indicating that the time series is exceedingly unpredictable.

It may be noted that Hurst exponent (H) mentioned here has been based on detrended fluctuation analysis (DFA). Hence, the results are not affected by local trends. As a future study, we propose the incorporation of further pollutants and a further comparison with the lockdown of 2021 due to the second wave.

Acknowledgements The authors express their sincere thankfulness to the anonymous reviewers for their constructive suggestions. Goutami Chattopadhyay is supported by DST, Govt. of India, under Project Grant No. SR/WOS-A/EA-10/2017(G).

Funding Department of Science and Technology, Ministry of Science and Technology, India, SR/WOS-A/EA-10/2017(G), Goutami Chattopadhyay

Data Availability Statement The data have been collected from the Central Pollution Control Board website, from where the link of http://cpcbenvis.nic.in/ is available.

References

1. F.A.B. Abdul Aziz, J. Mohd Ali, Tropospheric ozone formation estimation in urban city bangi using artificial neural network (ANN). Comput. Intell. Neurosci.. Intell. Neurosci. **19**(1), 6252983 (2019)
2. S.K. Allu, A. Reddy, S. Srinivasan, R.K. Maddala, G.R. Anupoju, Surface Ozone and its Precursor Gases Concentrations during COVID-19 Lockdown and Pre-Lockdown Periods in Hyderabad City, India. Environ. Processes **8**, 959 (2021)
3. D. Asimakopoulos, D. Deligiorgi, C. Drakopoulos, C. Helmis, K. Kokkori, D. Lalas, D. Sikiotis, C. Varotsos, An experimental study of nightime air-pollutant transport over complex terrain in Athens. Atmos. Environ. Part B. Urban Atmos. **26**(1), 59–71 (1992)
4. T. Banerjee, S.B. Singh, R.K. Srivastava, Development and performance evaluation of statistical models correlating air pollutants and meteorological variables at Pantnagar, India. Atmos. Res. **99**(3–4), 505–517 (2011)
5. B. Bera, S. Bhattacharjee, P.K. Shit, N. Sengupta, S. Saha, Significant impacts of COVID-19 lockdown on urban air pollution in Kolkata (India) and amelioration of environmental health. Environ. Dev. Sustain. **23**(5), 6913–6940 (2021)
6. B. Bera, S. Bhattacharjee, P.K. Shit, N. Sengupta, S. Saha, Variation and correlation between ultraviolet index and tropospheric ozone during COVID-19 lockdown over megacities of India. Stoch. Environ. Res. Risk Assess. **36**, 409 (2021)
7. A.D. Bhanarkar, S.K. Goyal, R. Sivacoumar, C.C. Rao, Assessment of contribution of SO2 and NO2 from different sources in Jamshedpur region, India. Atmos. Environ. **39**(40), 7745–7760 (2005)
8. C.D. Bray, A. Nahas, W.H. Battye, V.P. Aneja, Impact of lockdown during the COVID-19 outbreak on multi-scale air quality. Atmos. Environ. **254**, 118386 (2021)
9. N. Chakraborty, I. Mukherjee, A.K. Santra, S. Chowdhury, S. Chakraborty, S. Bhattacharya, A.P. Mitra, C. Sharma, Measurement of CO2, CO, SO2, and NO emissions from coal-based thermal power plants in India. Atmos. Environ. **42**(6), 1073–1082 (2008)
10. G. Chattopadhyay, S.K. Midya, S. Chattopadhyay, Information theoretic study of the ground-level ozone and its precursors over Kolkata, India, during the summer monsoon. Iran. J. Sci. Technol., Trans. A: Sci. **45**(1), 201–207 (2021)
11. G. Chattopadhyay, S.K. Midya, S. Chattopadhyay, MLP based predictive model for surface ozone concentration over an urban area in the Gangetic West Bengal during pre-monsoon season. J. Atmos. Solar Terr. Phys. **184**, 57–62 (2019)
12. G. Chattopadhyay, S. Chattopadhyay, R. Jain, Multivariate forecast of winter monsoon rainfall in India using SST anomaly as a predictor: neurocomputing and statistical approaches. Comptes Rendus. Géosci. **342**(10), 755–765 (2010)
13. R.R. Devi, S. Chattopadhyay, Multifractal detrended fluctuation analysis approach to the monthly total ozone concentration over New Delhi, India. Indian J. Phys. (2024). https://doi.org/10.1007/s12648-024-03204-5
14. R.R. Devi, S. Chattopadhyay, A modified multifractal detrended fluctuation analysis to study the precipitation across northeast India. Dyn. Atmos. Oceans. Atmos. Oceans **104**, 101402 (2023)
15. R. Checa-Garcia, M.I. Hegglin, D. Kinnison, D.A. Plummer, K.P. Shine, Historical tropospheric and stratospheric ozone radiative forcing using the CMIP6 database. Geophys. Res. Lett.. Res. Lett. **45**(7), 3264–3273 (2018)

16. A.B. Chelani, Study of extreme CO, NO2 and O3 concentrations at a traffic site in Delhi: statistical persistence analysis and source identification. Aerosol Air Qual. Res. **13**(1), 377–384 (2013)
17. Y. Chen, O. Wild, E. Ryan, S.K. Sahu, D. Lowe, S. Archer-Nicholls, Y. Wang, G. McFiggans, T. Ansari, V. Singh, R.S. Sokhi, Mitigation of PM 2.5 and ozone pollution in Delhi: a sensitivity study during the pre-monsoon period. Atmos. Chem. Phys. **20**(1), 499–514 (2020)
18. J. Cofala, M. Amann, F. Gyarfas, W. Schoepp, J.C. Boudri, L. Hordijk, C. Kroeze, L. Junfeng, D. Lin, T.S. Panwar, S. Gupta, Cost-effective control of SO2 emissions in Asia. J. Environ. Manag. **72**(3), 149–161 (2004)
19. A.P. Cracknell, C.A. Varotsos, The present status of the total ozone depletion over Greece and Scotland: a comparison between Mediterranean and more northerly latitudes. Int. J. Remote Sens. **16**(10), 1751–1763 (1995)
20. P.J. Crutzen, *Tropospheric ozone: an overview. Tropospheric ozone* (Springer, Cham, 1988), pp.3–32
21. M. Das, A. Das, R. Sarkar, S. Saha, A. Mandal, Examining the impact of lockdown (due to COVID-19) on ambient aerosols (PM 2.5): a study on Indo-Gangetic Plain (IGP) cities, India. Stoch. Environ. Res. Risk Assess. **35**, 1301 (2020)
22. S. Gautam, The influence of COVID-19 on air quality in India: a boon or inutile. Bull. Environ. Contam. Toxicol.. Environ. Contam. Toxicol. **104**(6), 724–726 (2020)
23. S.N. Ghosh, S.K. Midya, Atmospheric Ozone, its Depletion and Antartic Ozone Hole. Indian J. Phys. **68B**, 473 (1994)
24. S.D. Ghude, S.H. Kulkarni, C. Jena, G.G. Pfister, G. Beig, S.R.J. Fadnavisvan der A, Application of satellite observations for identifying regions of dominant sources of nitrogen oxides over the Indian Subcontinent. J. Geophys. Res.: Atmos. **118**(2), 1075–1089 (2013)
25. S.S. Gunthe, G. Beig, L.K. Sahu, Study of relationship between daily maxima in ozone and temperature in an urban site in India. Curr. Sci.. Sci. **110**, 1994–1999 (2016)
26. H.E. Hurst, R.P. Black, Y.M. Simaika, *The Nile Basin. Vol. XI. Nile Control Department, Ministry of Irrigation* (Cairo, Egypt, 1978)
27. P.K. Jana, S. Bhattacharyya, A. Banerjee, Effect of some climatic parameters on tropospheric and total ozone column over Alipore (22.52○ N, 88.33○ E) India. J. Earth Syst. Sci. **123**(7), 1653–1669 (2014)
28. P.K. Jana, S. Goswami, S.K. Midya, Short-term tropospheric ozone trend in India. Indian J. Phys. **86**(11), 951–960 (2012)
29. C. Johnson, J. Henshaw, G. Mclnnes, Impact of aircraft and surface emissions of nitrogen oxides on tropospheric ozone and global warming. Nature **355**(6355), 69–71 (1992)
30. N. Kalamaras, K. Philippopoulos, D. Deligiorgi, C.G. Tzanis, G. Karvounis, Multifractal scaling properties of daily air temperature time series. Chaos Solitons Fractals **98**, 38–43 (2017)
31. M.B. Karuppasamy, S. Seshachalam, U. Natesan, R. Ayyamperumal, S. Karuppannan, G. Gopalakrishnan, N. Nazir, Air pollution improvement and mortality rate during COVID-19 pandemic in India: global intersectional study. Air Qual. Atmos. Health **13**(11), 1375–1384 (2020)
32. X. Hu, W. Han, Y. Wang, K. Aunan, X. Pan, J. Huang, G. Li, Does air pollution modify temperature-related mortality? A systematic review and meta-analysis. Environ. Res. **210**, 112898 (2022)
33. M. Kaur, A.K. Nagpal, Evaluation of air pollution tolerance index and anticipated performance index of plants and their application in development of green space along the urban areas. Environ. Sci. Pollut. Res.Pollut. Res. **24**(23), 18881–18895 (2017)
34. I. Kayes, S.A. Shahriar, K. Hasan, M. Akhter, M.M. Kabir, M.A. Salam, The relationships between meteorological parameters and air pollutants in an urban environment. Global J. Environ. Sci. Manage **5**(3), 265–278 (2019)
35. N.A. Kgabi, R.M. Sehloho, Tropospheric ozone concentrations and meteorological parameters. Global J. Sci. Front. Res **12**, 11–21 (2012)
36. S.K. Kharol, V. Fioletov, C.A. McLinden, M.W. Shephard, C.E. Sioris, C. Li, N.A. Krotkov, Ceramic industry at Morbi as a large source of SO2 emissions in India. Atmos. Environ. **223**, 117243 (2020)
37. S.H. Kota, H. Guo, L. Myllyvirta, J. Hu, S.K. Sahu, R. Garaga, Q. Ying, A. Gao, S. Dahiya, Y. Wang, H. Zhang, Year-long simulation of gaseous and particulate air pollutants in India. Atmos. Environ. **180**, 244–255 (2018)
38. D.R. Kothawale, J.V. Revadekar, K.R. Kumar, Recent trends in pre-monsoon daily temperature extremes over India. J. Earth Syst. Sci. **119**(1), 51–65 (2010)
39. S. Lal, S. Venkataramani, M. Naja, J.C. Kuniyal, T.K. Mandal, P.K. Bhuyan, K.M. Kumari, S.N. Tripathi, U. Sarkar, T. Das, Y.V. Swamy, Loss of crop yields in India due to surface ozone: An estimation based on a network of observations. Environ. Sci. Pollut. Res.Pollut. Res. **24**(26), 20972–20981 (2017)
40. K.M. Lau, V. Ramanathan, G.X. Wu, Z. Li, S.C. Tsay, C. Hsu, R. Sikka, B. Holben, D. Lu, G. Tartari, M. Chin, The Joint Aerosol-Monsoon Experiment: A new challenge for monsoon climate research. Bull. Am. Meteor. Soc. **89**(3), 369–384 (2008)
41. H. Li, X.L. Xu, D.W. Dai, Z.Y. Huang, Z. Ma, Y.J. Guan, Air pollution and temperature are associated with increased COVID-19 incidence: a time series study. Int. J. Infect. Dis. **97**, 278–282 (2020)
42. C. Liu, H. Geng, P. Shen, Q. Wang, K. Shi, Coupling detrended fluctuation analysis of the relationship between O3 and its precursors–a case study in Taiwan. Atmos. Environ. **188**, 18–24 (2018)
43. A.L. Londhe, D.B. Jadhav, P.S. Buchunde, M.J. Kartha, Surface ozone variability in the urban and nearby rural locations of tropical India. Curr. Sci.. Sci. **95**, 1724–1729 (2008)
44. Z. Lu, D.G. Streets, B. de Foy, N.A. Krotkov, Ozone Monitoring Instrument observations of interannual increases in SO2 emissions from Indian coal-fired power plants during 2005–2012. Environ. Sci. Technol. **47**(24), 13993–14000 (2013)
45. S. Maithani, G. Nautiyal, A. Sharma, Investigating the Effect of Lockdown During COVID-19 on Land Surface Temperature: Study of Dehradun City, India. J. Indian Soc. Remote Sens. **48**(9), 1297–1311 (2020)
46. C. Mallik, S. Lal, M. Naja, D. Chand, S. Venkataramani, H. Joshi, P. Pant, Enhanced SO2 concentrations observed over northern India: role of long-range transport. Int. J. Remote Sens. **34**(8), 2749–2762 (2013)
47. C. Mallik, P.S. Mahapatra, P. Kumar, S. Panda, R. Boopathy, T. Das, S. Lal, Influence of regional emissions on SO2 concentrations over Bhubaneswar, a capital city in eastern India downwind of the Indian SO2 hotspots. Atmos. Environ. **209**, 220–232 (2019)
48. A. Manju, K. Kalaiselvi, V. Dhananjayan, M. Palanivel, G.S. Banupriya, M.H. Vidhya, K. Panjakumar, B. Ravichandran, Spatio-seasonal variation in ambient air pollutants and influence of meteorological factors in Coimbatore, southern India. Air Qual. Atmos. Health **11**(10), 1179–1189 (2018)
49. N. Mirzaei, H. Arfaeinia, M. Moradi, F. Mohammadi Moghadam, A. Velayati, K. Sharafi, The statistical analysis of seasonal and time variations on trend of important air pollutants (SO2, O3, NOx, CO, PM10)-in western Iran: a case study. Int. J. Pharm. Technol. **7**(3), 9610–9622 (2015)
50. M. Naja, C. Mallik, T. Sarangi, V. Sheel, S. Lal, SO2 measurements at a high altitude site in the central Himalayas: Role of regional transport. Atmos. Environ. **99**, 392–402 (2014)
51. C. Ogaugwu, H. Mogaji, E. Ogaugwu, U. Nebo, H. Okoh, S. Agbo, A. Agbon, Effect of Weather on COVID-19 Transmission and Mortality in Lagos, Nigeria. Scientifica **2020**, 2562641 (2020)
52. K. Padma, R.S. Selvaraj, B.M. Boaz, Use of Chaotic and Time Series Analysis on Surface Ozone Study at the Tropical Region, Chennai, Tamilnadu. Univ. J. Environ. Res. Technol. **3**(6), 650 (2013)

53. S. Panda, C. Mallik, J. Nath, T. Das, B. Ramasamy, A study on variation of atmospheric pollutants over Bhubaneswar during imposition of nationwide lockdown in India for the COVID-19 pandemic. Air Qual. Atmos. Health **14**(1), 97–108 (2021)
54. V. Pawar, S.D. Pawar, G. Beig, S.K. Sahu, Effect of lightning activity on surface NOx and O3 over a tropical station during premonsoon and monsoon seasons. J. Geophys. Res. Atmos. (2012). https://doi.org/10.1029/2011JD016930
55. D. Pudasainee, B. Sapkota, M.L. Shrestha, A. Kaga, A. Kondo, Y. Inoue, Ground level ozone concentrations and its association with NOx and meteorological parameters in Kathmandu valley, Nepal. Atmos. Environ. **40**(40), 8081–8087 (2006)
56. R.R. Reddy, K.R. Gopal, L.S.S. Reddy, K. Narasimhulu, K.R. Kumar, Y.N. Ahammed, C.K. Reddy, Measurements of surface ozone at semi-arid site Anantapur (14.62 N, 77.65 E, 331 m asl) in India. J. Atmos. Chem. **59**(1), 47–59 (2008)
57. S. Roberts, Interactions between particulate air pollution and temperature in air pollution mortality time series studies. Environ. Res. **96**(3), 328–337 (2004)
58. S. Roy, G. Beig, D. Jacob, Seasonal distribution of ozone and its precursors over the tropical Indian region using regional chemistry-transport model. J. Geophys. Res. Atmos. (2008). https://doi.org/10.1029/2007JD009712
59. A. Rathore, G.S. Gopikrishnan, J. Kuttippurath, Changes in tropospheric ozone over India: Variability, long-term trends and climate forcing. Atmos. Environ. **309**, 119959 (2023)
60. S. Rehman, A.H. Siddiqi, Wavelet based Hurst exponent and fractal dimensional analysis of Saudi climatic dynamics. Chaos Solitons Fractals **40**(3), 1081–1090 (2009)
61. D. Rupakheti, B. Adhikary, P.S. Praveen, M. Rupakheti, S. Kang, K.S. Mahata, M. Naja, Q. Zhang, A.K. Panday, M.G. Lawrence, Pre-monsoon air quality over Lumbini, a world heritage site along the Himalayan foothills. Atmos. Chem. Phys. **17**(18), 11041–11063 (2017)
62. M. Sarkar, A. Das, S. Mukhopadhyay, Assessing the immediate impact of COVID-19 lockdown on the air quality of Kolkata and Howrah, West Bengal, India. Environ. Dev. Sustain. **23**, 8613 (2020)
63. Y. Sathe, P. Gupta, M. Bawase, L. Lamsal, F. Patadia, S. Thipse, Surface and satellite observations of air pollution in India during COVID-19 lockdown: Implication to air quality. Sustain. Cities Soc. **66**, 102688 (2021)
64. F. Shahzad, U. Shahzad, Z. Fareed, N. Iqbal, S.H. Hashmi, F. Ahmad, Asymmetric nexus between temperature and COVID-19 in the top ten affected provinces of China: A current application of quantile-on-quantile approach. Sci. Total. Environ. **736**, 139115 (2020)
65. K. Shehzad, M. Sarfraz, S.G.M. Shah, The impact of COVID-19 as a necessary evil on air pollution in India during the lockdown. Environ. Pollut.Pollut. **266**, 115080 (2020)
66. M.K. Siddiqui, R. Morales-Menendez, P.K. Gupta, H.M. Iqbal, F. Hussain, K. Khatoon, S. Ahmad, Correlation between temperature and COVID-19 (suspected, confirmed and death) cases based on machine learning analysis. J. Pure Appl. Microbiol. **14**(suppl 1), 1017–1024 (2020)
67. J. Singh, B. Tyagi, Transformation of air quality over a coastal tropical station Chennai during COVID-19 lockdown in India. Aerosol Air Qual. Res. **21**, 200490 (2020)
68. A.K. Srivastava, P.D. Bhoyar, V.P. Kanawade, P.C. Devara, A. Thomas, V.K. Soni, Improved air quality during COVID-19 at an urban megacity over the Indo-Gangetic Basin: From stringent to relaxed lockdown phases. Urban Clim. **36**, 100791 (2021)
69. B. Tyagi, J. Singh, G. Beig, Seasonal progression of surface ozone and NOx concentrations over three tropical stations in North-East India. Environ. Pollut.Pollut. **258**, 113662 (2020)
70. D.L. Turcotte, *Fractals and chaos in geology and geophysics*, 2nd edn. (Cambridge University Press, Cambridge, 1997)
71. K.P. Vadrevu, A. Eaturu, S. Biswas, K. Lasko, S. Sahu, J.K. Garg, C. Justice, Spatial and temporal variations of air pollution over 41 cities of India during the COVID-19 lockdown period. Sci. Rep. **10**(1), 1–15 (2020)
72. C. Varotsos, Atmospheric pollution and remote sensing: implications for the southern hemisphere ozone hole split in 2002 and the northern mid-latitude ozone trend. Adv. Space Res. **33**(3), 249–253 (2004)
73. T. Viscek, *Fractal growth phenomena* (World Scientific, Singapore, 1989)
74. Z.S. Venter, K. Aunan, S. Chowdhury, J. Lelieveld, COVID-19 lockdowns cause global air pollution declines. Proc. Natl. Acad. Sci. **117**(32), 18984–18990 (2020)
75. D.S. Wilks, Resampling hypothesis tests for autocorrelated fields. J. Clim.Clim. **10**(1), 65–82 (1997)
76. H. Zhang, Y. Wang, J. Hu, Q. Ying, X.M. Hu, Relationships between meteorological parameters and criteria air pollutants in three megacities in China. Environ. Res. **140**, 242–254 (2015)